Coupled Systems Mechanics, *Vol. 6, No. 2 (2017) 113-125*
DOI: https://doi.org/10.12989/csm.2017.6.2.113

Heat transfer enhancement in gas tungsten arc welding using azimuthal magnetic fields generated by external current

Yiseul Kim[1], Jaewook Lee[*1], Xiaolong Liu[1], Boyoung Lee[1] and Yunlong Chang[2]

[1]Department of Aerospace and Mechanical Engineering, Korea Aerospace University, 76 Hanggongdaehang-ro, Deogyang-gu, Goyang-si, Gyeonggi-do, 412-791, Korea
[2]School of Materials Science and Engineering, Shenyang University of Technology, No. 111, Shenliao West Road, Economic & Technological Development Zone, Shenyang, 110870, P.R. China

(Received April 15, 2015, Revised September 20, 2015, Accepted October 1, 2015)

Abstract. This paper proposes the idea to enhance the heat transfer in Gas Tungsten Arc Welding (GTAW) by using the azimuthal magnetic field. The azimuthal magnetic field generated by the external currents makes the Lorentz force stronger, and consequently improves the heat transfer by the faster flow movement. The enhanced heat transfer might improve the welding performance by increasing the temperature at the workpiece. To validate the proposed idea, a two-dimensional axi-symmetric model of GTAW is built, and the multiphysics simulation of GTAW is carried out. As the analysis result, the distributions of electric current, electromagnetic fields, arc flow velocity, and temperature are investigated. Then, the proposed idea for heat transfer enhancement is validated by comparing the Lorentz force, flow velocity, and temperature distribution with and without azimuthal magnetic fields.

Keywords: thermal plasma; finite element analysis; electromagnetic fields; fluid dynamics; heat transfer; azimuthal magnetic fields

1. Introduction

Due to its high welding quality, the Gas Tungsten Arc Welding (GTAW), also known as Tungsten Inert Gas (TIG) welding has been extensively used in the manufacturing industry. To understand the behavior of GTAW, multiphysics simulation including electromagnetic fields, fluid dynamics, and heat transfer is inherently required. Due to the complexity of a system of governing equations in GTAW, it is difficult to predict the behavior based on the experiment or the analytical approach. Thus, the numerical simulation has been vigorously performed. Two dimensional axi-symmetric model was developed to describe heat transfer and fluid flow by Fan and Shi (1996), Wu *et al*. (1997). The developed model was used for the case of gas mixture of argon and hydrogen (Lowke *et al*. 1997). Lu *et al*. (2004) established the mathematical model for not only GTAW arc, but also weld pool. The simulation approaches were validated by comparing with the experimental results under various kinds of shielding gas (Savas and Ceyhun 2011). Varghese (2013) reviewed the developed model for the numerical simulation of GTAW.

*Corresponding author, Assistant Professor, E-mail: wookslee@kau.ac.kr

http://www.techno-press.org/?journal=csm&subpage=8 ISSN: 2234-2184 (Print), 2234-2192 (Online)

Based on the developed mathematical models, various attempts to improve the welding performance have been carried out by identifying the influence of GTAW design variables. The effect of cathode tip angle on the welding properties was investigated by Goodarzi *et al*. (1997). Du *et al*. (2009) identified the influence of input current, flow rate and kinds of shielding gas, arc length on the arc properties such as temperature, velocity, and current were studied. To improve the GTAW welding performance, helium addition into shielding gas were proposed, and the energy transfer enhancement was shown by using numerical simulation (Traidia and Roger 2011). A two-electrode GTAW was proposed to increase the arc temperature by Ding *et al*. (2014).

In this paper, the new concept to enhance the heat transfer in GTAW is proposed using the azimuthal magnetic fields generated by upward direction external current. Previously, the influence of the axial direction magnetic fields was investigated by Yin *et al*. (2012). They discovered the change of radial spread and weld pool by applied magnetic fields. However, the axial direction magnetic field might not directly improve the heat transfer. Here, the azimuthal magnetic field by upward direction external current is proposed for the straightforward enhancement of the heat transfer. In GTAW, most of heat is generated near the tip of cathode. The generated heat is transferred to workpiece by arc flow driven by the Lorentz force. Thus, the increase of the Lorentz force might raise the temperature of the workpiece by the faster arc flow velocity. To increase the Lorentz force, the azimuthal magnetic fields by the external current is proposed considering the direction of current, magnetic field and Lorentz force. To validate the proposed idea, the two-dimensional axi-symmetric model of GTAW is built and multiphysics simulation is performed. The effect of azimuthal magnetic fields on the temperature in the workpiece is investigated by comparing the GTAW characteristics with and without external current. The current density distribution, electric and magnetic field distributions and arc velocity and temperature distribution are compared, and the mechanism of the temperature raise in the workpiece is identified.

The remained sections of the paper are organized as follows. Section 2 describes the multiphysics modeling of GTAW by investigating a system of governing equations and boundary conditions. Section 3 explains the proposed idea for heat transfer enhancement by azimuthal magnetic fields generated by upward external current. The simulation results with and without azimuthal magnetic fields are compared to validate the proposed idea in Section 4. Finally a conclusion is provided in Section 5.

2. Multiphysics modeling of GTAW

2.1 Problem formulation

This section explains multiphysics simulation to understand plasma's behavior in GTAW. Fig. 1(a) shows the schematic figure of GTAW, and its two-dimensional axi-symmetric model is presented in Fig. 1(b). In GTAW, Non-consumable tungsten is used as the cathode and workpiece becomes the anode. A potential difference between the cathode and anode generates the electric current between them. The high DC power of the cathode makes shielding gas ionized near the top of cathode. The fully ionized shielding gas having the electric conductivity is concentrated into the cathode driven by the electromagnetic force. Then, the gas transfers the generated heat from the cathode to the anode. To understand the physical phenomenon of GTAW, the multiphysics analysis including electromagnetic fields, fluid flow and the heat transfer is required. It is hard to

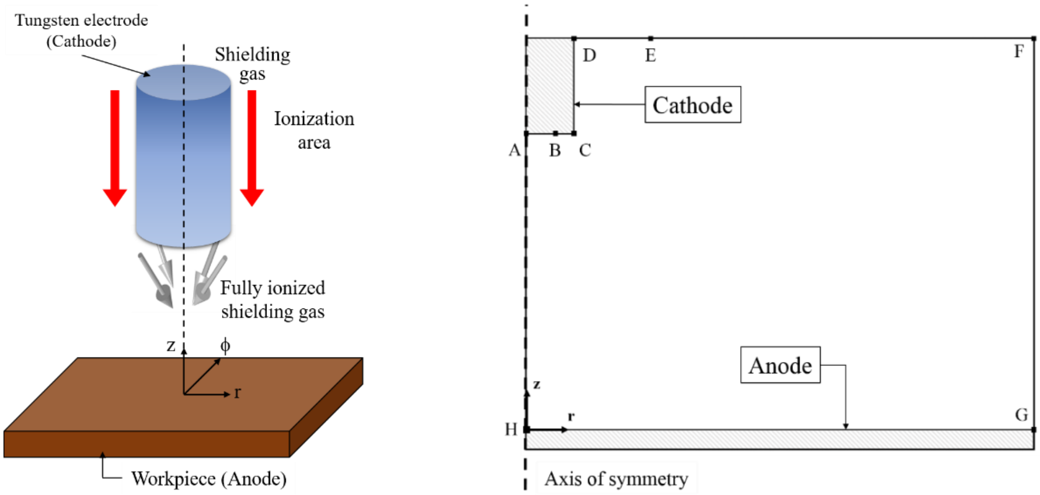

(a) (b)

Fig. 1(a) Schematic figure of GTAW, (b) 2D Axi-symmetric model of GTAW

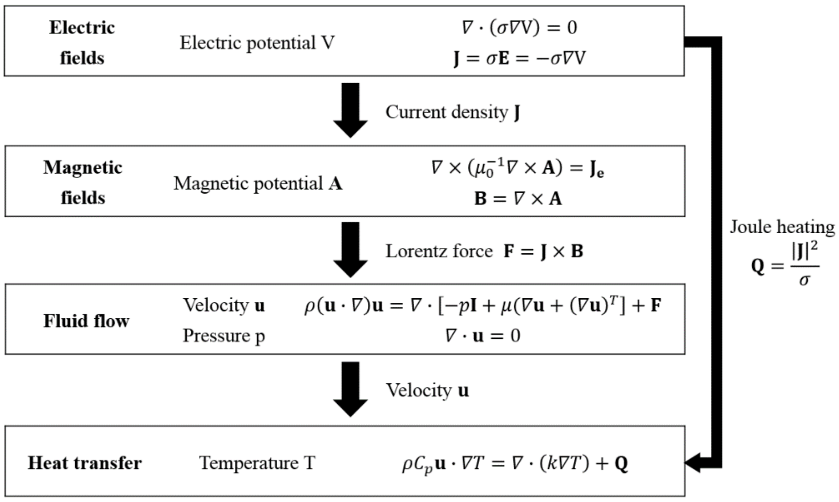

Fig. 2 The flowchart of governing equations

consider the whole physical phenomenon including the ionization of shielding gas. Thus, we assume that shielding gas is fully ionized for the simplicity.

2.2 Flow chart of multiphysics simulation in GTAW

Fig. 2 presents the flowchart of the multiphysics analysis in GTAW. The figure shows the weakly coupled governing equations and corresponding state variables. The physical parameters used in Fig. 2 is explained in Table 1. The electromagnetic force generated by the current and the magnetic field drives the flow motion of shielding gas. By this gas flow, the heat produced by the current from the cathode is transferred into anode. In other words, the electromagnetic fields

Table 1 Symbols

V	Electric potential	u	Velocity
J	Current density	p	pressure
E	Electric fields	ρ	Density
σ	Electrical conductivity	μ	Viscosity
A	Magnetic vector potential	C_p	Heat capacity
μ_o	Magnetic permeability of free space	T	Temperature
J_e	External current	k	heat conductivity
B	Magnetic fields		

generates the heat and electromagnetic force that drive the arc flow. The Lorentz force generated by the electromagnetic fields is included as the volume force in the fluid flow equations. Joule heating term is included in heat transfer equation as heat source term. The detailed explanation for each physics will be explained in Section 2.4.

2.3 Assumptions

The computational domain is symmetric about the *z*-axis. We solved the problem in steady-state. The plasma is stable and the fully ionized gas flows to domain. The gas flow is laminar and incompressible flow. Most important assumption is the plasma is in Local thermal equilibrium (LTE) and the plasma in LTE is called thermal plasma. In heat transfer, we ignore the additional heat source term except the Joule heating. Although the radiation loss and electron flux effect is important, we need to make the problem simple for the design.

2.4 Governing equations

2.4.1 Electromagnetic fields

Electromagnetic fields can be expressed by Maxwell's equations. We use the potential formulation. The current continuity equation is

$$\frac{\partial}{\partial \mathrm{z}}\left(\sigma \frac{\partial V}{\partial z}\right)+\frac{1}{r}\frac{\partial}{\partial r}\left(r\sigma\frac{\partial V}{\partial r}\right)=0 \tag{1}$$

We can get the current density by calculating the gradient of electric potential. The Ohm's law equations are

$$\mathrm{J_z}=-\sigma\frac{\partial V}{\partial z},\ \mathrm{J}_r=-\sigma\frac{\partial V}{\partial r} \tag{2}$$

J_r and J_z are the radial and axial components of current density. Magnetic potential equations are

$$\frac{\partial^2 A_z}{\partial z^2}+\frac{1}{r}\frac{\partial}{\partial r}\left(r\frac{\partial A_z}{\partial r}\right)=\mu_0 J_z \tag{3}$$

$$\frac{\partial^2 A_r}{\partial z^2}+\frac{1}{r}\frac{\partial}{\partial r}\left(r\frac{\partial A_r}{\partial r}\right)-\frac{A_z}{r^2}=\mu_0 J_r \tag{4}$$

A_r and A_z are the radial and axial components of magnetic potential. We can get the magnetic fields by calculation the curl of magnetic potential. The azimuthal component of magnetic fields is

$$\mathrm{B}_{\theta} = \frac{\partial A_r}{\partial z} - \frac{\partial A_z}{\partial r} \tag{5}$$

2.4.2 Fluid flow

The fluid flow equation set are presented. Mass conservation equation is

$$\frac{\partial}{\partial z}(\rho \mathrm{v}) + \frac{1}{r}\frac{\partial}{\partial r}(\rho r \mathrm{u}) = 0 \tag{6}$$

u and v are velocity of axial and radial components respectively. Momentum conservation equations are

-Radial direction

$$\frac{\partial}{\partial \mathrm{z}}(\rho v u) + \frac{1}{r}\frac{\partial}{\partial r}(\rho r u u) = -\frac{\partial P}{\partial r} + \frac{\partial}{\partial z}\left(\mu\frac{\partial u}{\partial z} + \mu\frac{\partial v}{\partial r}\right) + \frac{1}{r}\frac{\partial}{\partial r}\left(2r\mu\frac{\partial u}{\partial r}\right) - J_z B_{\phi} \tag{7}$$

-Axial direction

$$\frac{\partial}{\partial \mathrm{z}}(\rho v v) + \frac{1}{r}\frac{\partial}{\partial r}(\rho r u v) = -\frac{\partial P}{\partial z} + \frac{1}{r}\frac{\partial}{\partial r}\left(r\mu\frac{\partial v}{\partial r} + r\mu\frac{\partial u}{\partial z}\right) + \frac{\partial}{\partial z}\left(2\mu\frac{\partial v}{\partial z}\right) + J_r B_{\phi} \tag{8}$$

The above momentum conservation equations are different from the classical momentum conservation equations. There is force term generated by ‘Lorentz force. We can get the radial and axial components of Lorentz force by calculating ‘$J \times B$’. The detail about Lorentz force will be explained next section.

2.4.3 Heat transfer

Energy conservation equation is

$$\frac{\partial}{\partial \mathrm{z}}\left(\rho v C_p T\right) + \frac{1}{r}\frac{\partial}{\partial r}\left(\rho r u C_p T\right) = \frac{\partial}{\partial z}\left(k\frac{\partial T}{\partial z}\right) + \frac{1}{r}\frac{\partial}{\partial r}\left(rk\frac{\partial T}{\partial r}\right) + \frac{J_z^2 + J_r^2}{\sigma} \tag{9}$$

The last term is the Joule heating term generated by electrode.

2.5 Boundary conditions

This section gives boundary conditions in briefly. More specific explanation is made in this reference. (Savas and Ceyhun 2011)

-Electromagnetic fields

Magnetic insulation condition is applied in all boundaries. For the electric potential, outward normal current density condition is set on electrode area and ground condition is set on workpiece. We set the cathode current as 200(A), and the current density at the cathode is 6.7×10^{7}(A/m^{2}). The electrical insulation condition is set on the rest of boundaries.

-Fluid flow

Pure argon gas is used for shielding gas and flows through DE boundary. Line EF, FG boundary condition is the atmospheric pressure condition.

-Heat transfer

The constant temperature condition is set on electrode part and open part. The rest of boundary, the workpiece is thermal insulation condition.

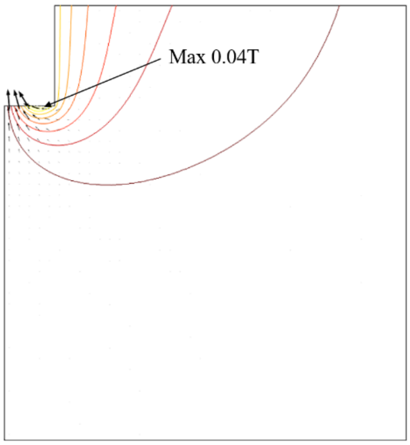

Fig. 3 The azimuthal direction of magnetic flux density (contours, interval: 0.005T) and The current density (arrow line)

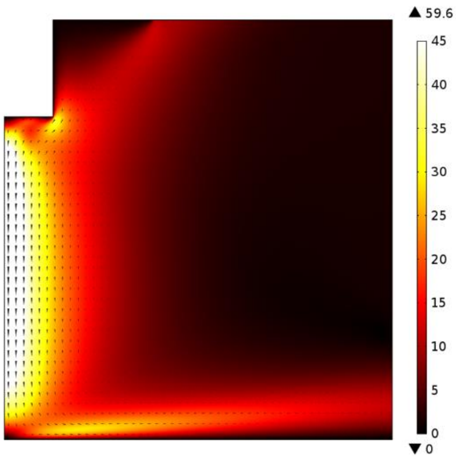

Fig. 4 The velocity fields surface and contours (max: 60, min: 15, interval: 9 m/s)

2.6 Numerical method

We solved the problem using the commercial software ‘COMSOL 4.4’. This problem has high instability in fluid equations. So we build the fine mesh. Number of degree of freedom is about 340000. It takes about 5 minute for solving the problem.

Fig. 3 is plot of the azimuthal direction of magnetic flux density and the current density. Potential difference between the electrode and the workpiece makes the radial and axial components of current density and this makes the azimuthal direction of self-induced magnetic fields.

Fig. 4 is the velocity fields. It says that the conductive gas flow is driven by Lorentz force under the tip. This shows that the gas inflows inlet near the tip and moves to the center area under the electrode. It make the arc column. The gas flows to the workpiece and outflows along the workpiece surface.

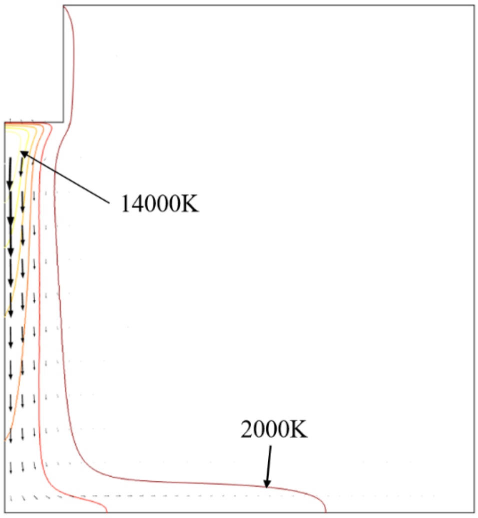

Fig. 5 The isothermal contours (interval: 2000 K) and the total heat flux (arrow line)

Fig. 5 is the isothermal contours and the total heat flux (arrow line). The maximum value is 14000 K and minimum value is 2000 K. To see the total heat flux, the heat generated by electrode is transferred to workpiece. The total heat flux has high value where the gas velocity is high. And the area of high total heat flux has dense temperature contours.

Comparing the above results and equations, this model can obtain physically reasonable results.

3. Magnetic fields manipulation

In welding, heat transfer have to be high at workpiece (anode) for increasing the performance. Arc column have to be narrow and high temperature have to be concentrated along the arc length for increasing the temperature at workpiece. For this goal, we need to make the heat transfer improved. Because improving the heat transfer is that the heat generated by electrode is well transferred to workpiece. To improve the heat transfer, the velocity of fluid flow have to be high. Because Fig. 4 and Fig. 5 say that the high velocity area has the high total heat flux and the rapidly changed temperature contours. The fluid flow is responding to the Lorentz force. This makes the arc column shrink. The force which effect on the velocity fields being fast is the radial and axial components of Lorentz force.

The Lorentz force can be expressed as

$$F = J \times B = (j_\phi B_z - j_z B_\phi)\hat{e}_r + (j_r B_\phi - j_\phi B_r)\hat{e}_z - (j_r B_z - j_z B_r)\hat{e}_\phi \tag{10}$$

In this problem, the azimuthal component of current density is zero. Therefore the Eq. (10) will be written as

$$F = -(j_z B_\phi)\hat{e}_r + (j_r B_\phi)\hat{e}_z - (j_r B_z - j_z B_r)\hat{e}_\phi \tag{11}$$

According to the Eq. (11) and Fig. 6, the azimuthal component of magnetic fields have an effect on the radial and axial components of Lorentz force. Therefore we realized that the

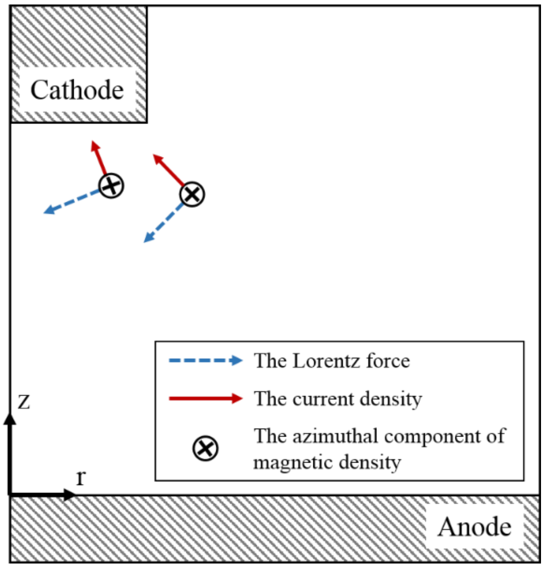

Fig. 6 Schematic figure of interaction between the current density, magnetic density and Lorentz force

azimuthal component of magnetic fields has to be increased to make the velocity fast.

Fig. 7 is the conceptual figure of the magnetic fields improvement. The coil is added to original system and the external current is set. This external current makes the additional magnetic fields. According to the above referred Eq. (11), the azimuthal component of magnetic fields have to be changed. Therefore the axial component of the current density have to be set for this change. We realized that integration of the magnetic fields generated by coil and the cathode results in the stronger Lorentz force than original system. The velocity of fluid flow driven by the Lorentz force will be faster.

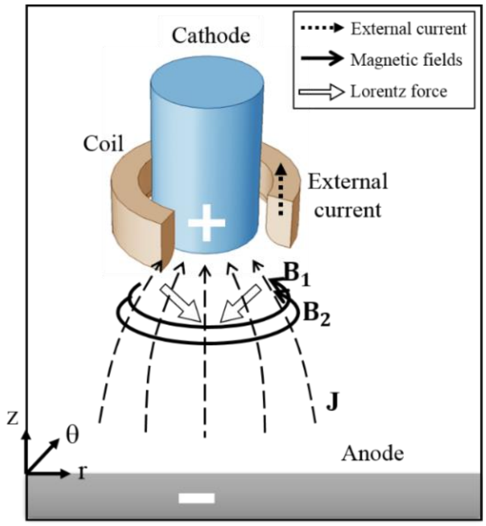

Fig. 7 Conceptual diagram of electromagnetic viewpoint of the coil added welding system

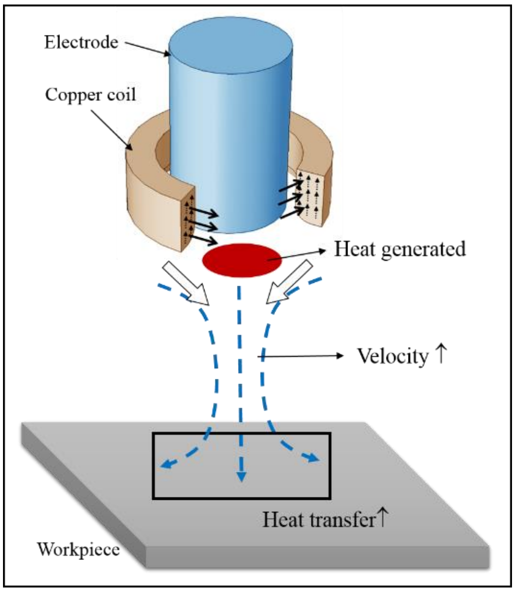

Fig. 8 The diagram of the coil added welding system

Fig. 8 is the diagram of the physical situation of the coil added welding system. The heat generated by electrode is transferred by the fluid flow. Because of the improvement of the Lorentz force, gas flow velocity is higher than the original system. Fast gas flow transfers the heat better. As a result, the heat flux will be raised and the heat transfer will be improved at the workpiece.

Fig. 9 is the computational domain of coil added system. Coil is set next to cathode. The axial direction of external current is set to coil.

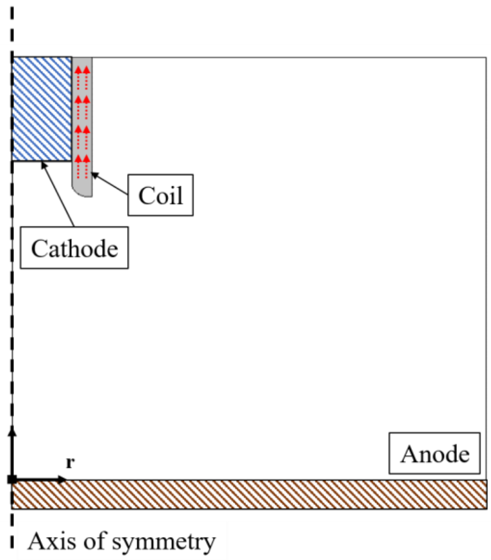

Fig. 9 Computational domain of the coil added system

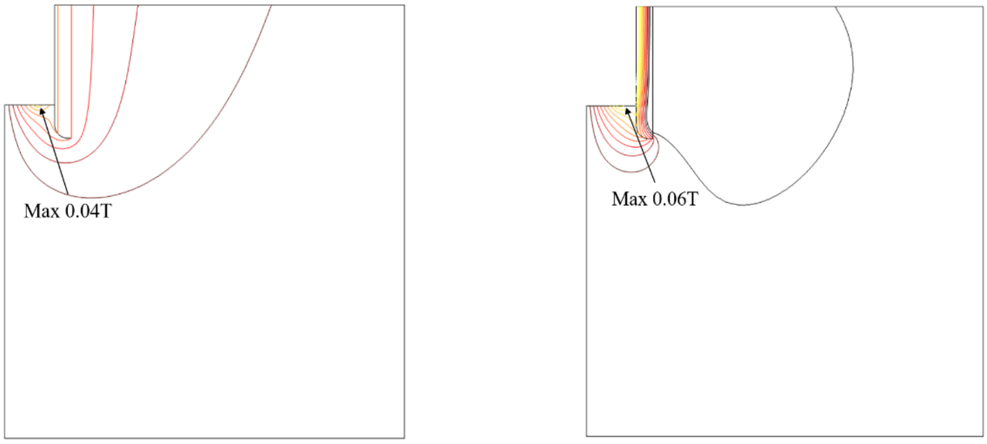

(a) No external current (b) External current

Fig. 10 The azimuthal component of magnetic flux density contours (interval: 0.005 T)

4. Result and discussion

For the accurate comparison, we compare the two results. Because we want to check whether the coil structure effects on the result. One is just added coil, no external current density. Another one has external current density. For the external azimuthal coils, we set the current as 12A. The number of turns for the external coil is 50, and the current density is 10.0×10^{7} A/m^{2}.

Fig. 10 is the azimuthal component of magnetic flux density contours. No external case has similar magnetic flux density contours with original system. (see Fig. 3 and Fig. 10(a)) The external current case has higher maximum value and dense magnetic flux density contours, which is shown in Fig. 10(b). This result says that additional external current, especially the axial direction current, makes the azimuthal direction of magnetic flux density stronger.

Fig. 11 is the Lorentz force arrow line. The longer length of the arrow line is, the stronger magnitude of the Lorentz force is. This figure shows that the black arrow lines which present the external current case are bigger than the red arrow lines which present the no external current case. Therefore we can realize that the Lorentz force increased responding to magnetic flux density increasing.

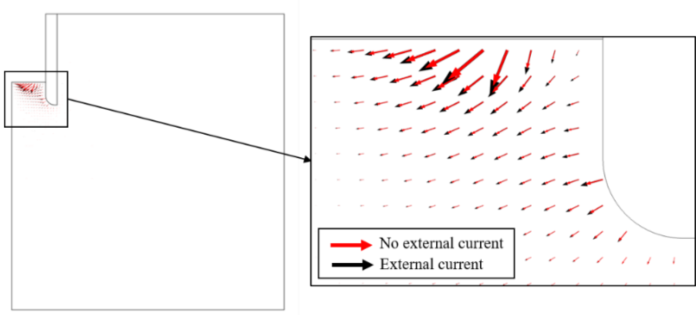

Fig. 11 The Lorentz force arrow surface

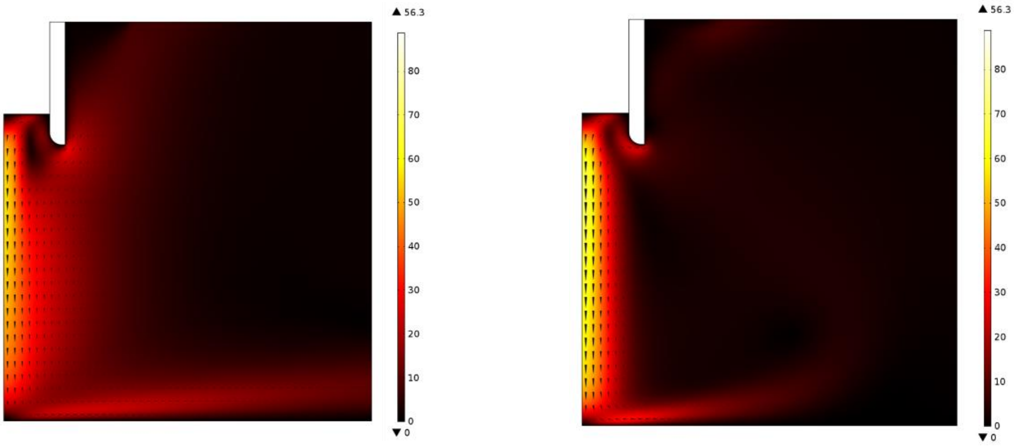

(a) No external current (b) External current

Fig. 12 The velocity fields and equivalence contour (max: 70, min: 10, interval: 12 m/s)

Fig. 12 shows the velocity fields in the same scale. External current case has higher value near the axis of symmetry. And this result is shown that the maximum value is increased about 20% comparing the no external current case. Velocity fields of two case have to be same if the Lorentz force doesn't work to gas flow. But the velocity is changed responding to the Lorentz force. Therefore we expect that the velocity is increased by the Lorentz force not the effect of coil structure.

Fig. 13 is the isothermal contour and total heat flux plot. The total heat flux is improved because of the fasten velocity. As a result the temperature in workpiece is increased. The higher temperature contour value comes down toward workpiece comparing the Fig. 13(a)-(b). This implies that the heat in the external current case is transferred better to the workpiece than the no external current case.

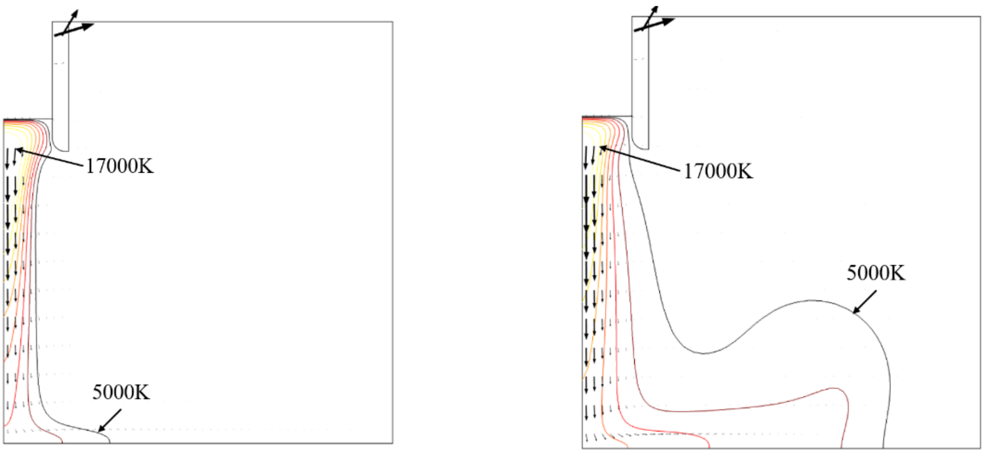

(a) No external current (b) External current

Fig. 13 The isothermal contours (interval: 1500 K) and total heat flux (arrow line)

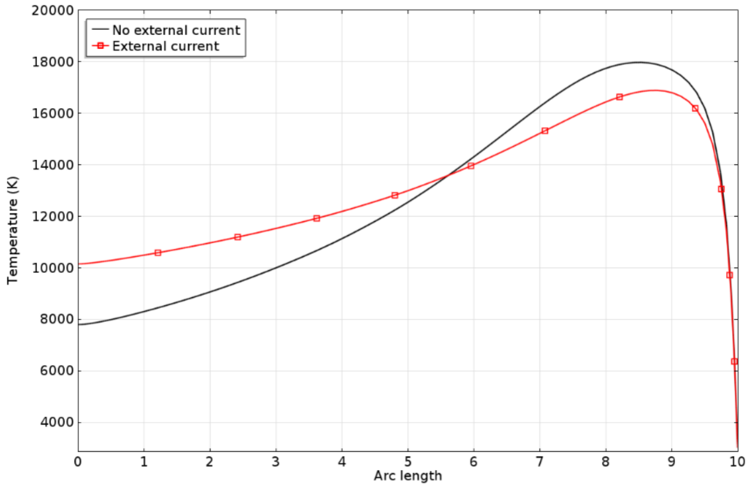

Fig. 14 The temperature plot along the arc length

More accurate result is shown in Fig. 14. This is the temperature plot along the arc length under the center of the electrode. At the workpiece, the temperature is increased about 25% and this results says that the magnetic field manipulations works to improvement of heat transfer.

5. Conclusions

The addition of the external current in GTAW is proposed to improve the heat transfer performance of GTAW. The azimuthal magnetic field generated by upward direction external current makes the Lorentz force stronger, and consequently improve the heat transfer by the faster flow velocity. Multiphysics simulation model is built to verify the proposed idea. The comparison of Lorentz force, flow velocity, and temperature distribution with and without external current validates that the azimuthal magnetic field might improve the GTAW performance.

Acknowledgments

This research was supported by Basic Science Research Program through the National Research Foundation of Korea (NRF) funded by the Ministry of Education (No.2013R1A1A2058086).

References

Ding, X., Li, H., Yang, L., Gao, Y. and Wei, H. (2014), "Numerical analysis of arc characteristics in two-electrode GTAW", *Int. J. Adv. Manuf. Technol.*, **70**(9-12), 1867-1874.

Du, H., Wei, Y., Wang, W., Lin, W. and Fan, D. (2009), "Numerical simulation of temperature and fluid in GTAW-arc under changing process condition", *J. Mater. Process. Technol.*, **209**(8), 3752-3765.

Fan, H.G. and Shi, Y.W. (1996), "Numerical simulation of the arc pressure in gas tungsten arc welding", *J. Mater. Process. Technol.*, **61**(3), 302-308.

Goodarzi, M., Choo, R. and Toguri, J.M. (1997), "The effect of the cathode tip angle on the GTAW arc and weld pool: I. Mathematical model of the arc", *J. Phys. D: Appl. Phys.*, **30**(19), 2744-2756.

Lowke, J.J., Morrow, R., Haidar, J. and Murphy, A.B. (1997), "Prediction of gas tungsten arc welding properties in mixture of argon and hydrogen", *IEEE Trans. Plasma Sci.*, **25**(5), 925-930.

Traidia, A. and Roger, F. (2011), "A computational investigation of different helium supplying methods for the improvement of GTA welding", *J. Mater. Process. Technol.*, **211**(9), 1553-1562.

Savas, A. and Ceyhun, V. (2011), "Finite element analysis of GTAW arc under different shielding gases", *Comput. Mater. Sci.*, **51**(1), 53-71.

Varghese, V.M.J., Suresh, M.R.D. and Kumar, S. (2013), "Recent developments in modeling of heat transfer during TIG weldin", *Int. J. Adv. Manuf. Technol.*, **64**(5-8), 749-754.

Wu, C.S., Ushio, M. and Tanaka, M. (1997), "Analysis of the TIG welding arc behavior", *Comput. Mater. Sci.*, **7**(3), 308-314.

Yin, X., Gou, J., Zhang, J. and Sun, J. (2012), "Numerical study of arc plasma and weld pools for GTAW with applied axial magnetic fields", *J. Phys. D: Appl. Phys.*, **45**(28), 285203.

MC